Asymmetric Transceiver Phased Array for Functional Imaging and Spectroscopy of the Visual Cortex at 9.4 T

Nikolai I Avdievich[1], Ioannis A Giapitzakis[1], and Anke Henning[1,2]

[1]*Max Planck Institute for Biological Cybernetics, Tübingen, Germany,* [2]*Institute for Biomedical Engineering, UZH and ETH Zurich, Zurich, Switzerland*

Introduction: Ultra-high (≥7T) field (UHF) functional magnetic resonance imaging (fMRI) and magnetic resonance spectroscopy (MRS) benefit from high SNR, BOLD contrast and spectral resolution. However, designing UHF RF coils is very challenging due to limitations, which include decreased transmit (Tx) efficiency ($B_1^+/\sqrt{P}$) and distorted B_1^+ field profile due to interaction with conductive dielectric tissue (1,2). For applications of high resolution fMRI and functional MRS (fMRS) in the visual cortex an open RF coil structure is highly suitable since it provides space for stimulation equipment, allows maximizing the Tx efficiency by focusing the RF field in a small localized area and obtains high SNR due to its close proximity. **In this work**, we demonstrate that an asymmetric transceiver (Tx/Rx) array design achieves optimal coverage of the posterior brain for both transmission and reception as needed for fMRI and fMRS of the visual cortex at 9.4T. The novel design is compared to a previous symmetric design (3).

Methods: A previously developed 4-channel surface loop Tx/Rx phased array (8.5cm - length) covered symmetrically a 150º arc on a 16.5cm diameter holder (Fig.1A) (3). Experimental transverse B_1^+ maps (Fig.1B) show a strong counter clockwise (CCW) twist (1), which decreases the B_1^+ near the central axis, while the receive (Rx) profile (B_1^-) of each loop is twisted clockwise (CW) (1). Rotating the entire array CW (Fig.1C) makes the B_1^+ profile more symmetrical. However a CW rotated array produces an even stronger CW twist of the B_1^- pattern reducing the SNR near loop #4 as well as the contribution of loop #1 to the SNR in the visual cortex. Thus a CCW rotated Rx array based on channels 2-4 and an additional Rx-only channel 5 (Fig.1C) would be optimal for reception. To prove the concept of opposite (CW and CCW) rotation of Tx and Rx arrays to improve coverage of the occipital brain we utilized an existing larger (23cm x 20cm, 10cm - length) 8-channel Tx/Rx array (4) using only 5 bottom loops (Fig.1C). Loops 1-4 were used for transmission, while loops 2-5 were used for reception. The larger size of the "5-channel" array also allows for variation of the penetration depth, which is determined by the array size and the phase shift between the loops. B_1^+ maps were obtained using the AFI sequence (5) and a head/shoulder (HS) phantom (Fig.1A,C) constructed to match tissue properties (ε=58.6, σ=0.64 S/m) (2). Data were acquired on a Siemens Magnetom whole body 9.4T human MRI system. EM-simulation based SAR estimation was performed using CST Studio Suite and the Virtual Family "Duke" model.

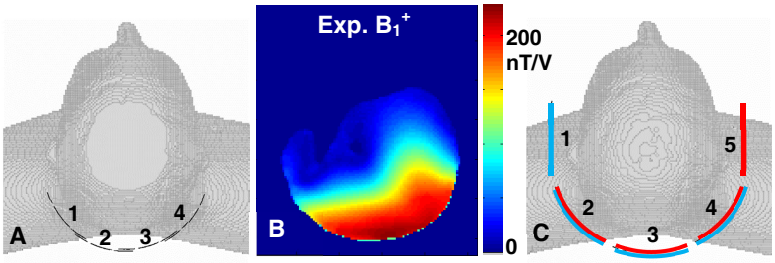

Fig.1: *A) view of the symmetric 4-ch. array; B) B_1^+ map obtained using the symmetric 4-ch. array and HS phantom with 90º phase shift b/w the loops; C) view of the "5-channel" array with Rx (red) and Tx (blue) elements shown.*

Results: Figs.2A,B show experimental and simulated B_1^+ maps of the central transversal slice obtained using the asymmetric 5-channel array and the HS phantom. Fig.2C shows an in-vivo B_1^+ map of the central transversal slice. All maps were obtained with 90º phase shift b/w adjacent loops. Experimental and simulated data match well and demonstrate good left-right symmetry. Table1 summarizes data including local SAR and Tx efficiency evaluated as $<B_1^+>/\sqrt{kW}$ and $<B_1^+>/\sqrt{SAR}$ ratio. B_1^+ averaging was performed over an ROI with the RF field greater than 40% of the maximum value. In-vivo efficiency (Fig.1C) measured 21.5 μT/√kW. Fig.2D shows plots along the central line of transversal B_1^+ maps obtained experimentally using the smaller 4-channel and the larger asymmetric 5-channel arrays with 45º and 90º phase shifts b/w adjacent loops. Decreasing the array size (loops, holder) allows increasing B_1^+ at the price of smaller penetration depth. Increase of the phase shifts b/w the loops decreases the penetration depth but increases B_1^+ as well as the local SAR. Finally, Fig.2E shows the SNR of the SoS-combined image of the HS phantom also demonstrating good symmetry.

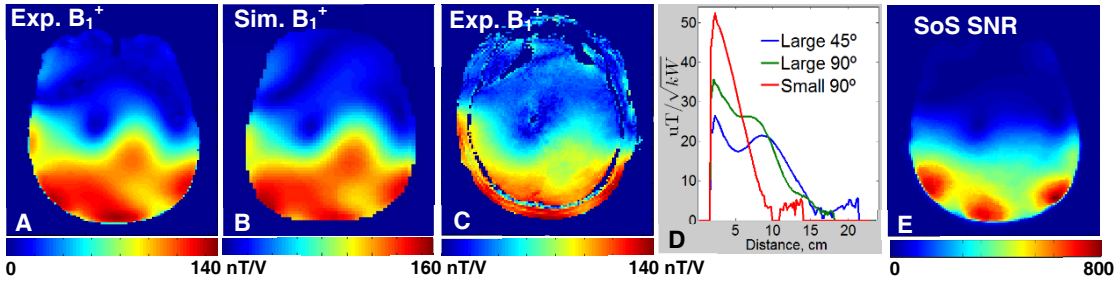

Fig.2: *Experimental (A), simulated (B) B_1^+ transversal maps from HS phantom; C) In-vivo transversal B_1^+ map (5-ch. array, 90º phase shift). D) Plots along the central line of the transversal B_1^+ maps for the 4-ch. (small) and 5-ch. (large) arrays; E) SNR of the SoS GE image of the SH phantom.*

Size, Phase	$<B_1^+>$ μT/√kW	*SAR_{10G} W/kG	$<B_1^+>/\sqrt{SAR}$ ratio
Sm.45º	33.9	1.69	1.31
Sm.90º	37.3	1.98	1.33
L.45º	19.8	0.98	1
L.90º	23.1	1.57	0.92

Table 1. * calculated for P_{in}= 1W at the coil.

Conclusions: We demonstrate that at 9.4T the 5-channel open phased array with asymmetric arrangement of 4 CW rotated Tx and 4 CCW rotated Rx elements improves the B_1^+ profile without compromising the B_1^- distribution. We also evaluated changes in the Tx efficiency, penetration depth and local SAR due to variation in the array size and the phase shift between the elements.

References: 1) Collins CM et al, MRM, 47:1026-1028, 2002. 2) Shajan G et al, MRM, 71:870-879, 2014. 3) Pfrommer A, Proc. ISMRM 2014, 1305. 4) Avdievich NI et al, Proc. ISMRM 2014. 5) Pohmann R, Scheffler K, NMR in Biomed, 26:265, 2013.